

N-ethyl-N-nitrosourea-based generation of mouse models for mutant G protein-coupled receptors

Johannes Grosse, Patrick Tarnow, Holger Römpler, Boris Schneider, Reinhard Sedlmeier, Ulrike Huffstadt, Dirk Korthaus, Michael Nehls, Sigrid Wattler, Torsten Schöneberg, Heike Biebermann and Martin Augustin

Physiol Genomics 26:209-217, 2006. First published May 23, 2006;
doi:10.1152/physiolgenomics.00289.2005

You might find this additional information useful...

Supplemental material for this article can be found at:

<http://physiolgenomics.physiology.org/cgi/content/full/00289.2005/DC1>

This article cites 54 articles, 15 of which you can access free at:

<http://physiolgenomics.physiology.org/cgi/content/full/26/3/209#BIBL>

Updated information and services including high-resolution figures, can be found at:

<http://physiolgenomics.physiology.org/cgi/content/full/26/3/209>

Additional material and information about *Physiological Genomics* can be found at:

<http://www.the-aps.org/publications/pg>

This information is current as of February 9, 2007 .

N-ethyl-*N*-nitrosourea-based generation of mouse models for mutant G protein-coupled receptors

Johannes Grosse,¹ Patrick Tarnow,² Holger Römpler,³ Boris Schneider,¹ Reinhard Sedlmeier,¹ Ulrike Huffstadt,¹ Dirk Korthaus,¹ Michael Nehls,¹ Sigrid Wattler,¹ Torsten Schöneberg,³ Heike Biebermann,² and Martin Augustin¹

¹Ingenium Pharmaceuticals AG, Martinsried; ²Charité Campus Virchow Klinikum, Institute of Pediatric Endocrinology, Humboldt University, Berlin; and ³Institute of Biochemistry, Molecular Biochemistry, Medical Faculty, University of Leipzig, Leipzig, Germany

Submitted 23 November 2005; accepted in final form 10 May 2006

Grosse, Johannes, Patrick Tarnow, Holger Römpler, Boris Schneider, Reinhard Sedlmeier, Ulrike Huffstadt, Dirk Korthaus, Michael Nehls, Sigrid Wattler, Torsten Schöneberg, Heike Biebermann, and Martin Augustin. *N*-ethyl-*N*-nitrosourea-based generation of mouse models for mutant G protein-coupled receptors. *Physiol Genomics* 26: 209–217, 2006. First published May 23, 2006; doi:10.1152/physiolgenomics.00289.2005.—Chemical random mutagenesis techniques with the germ line supermutagen *N*-ethyl-*N*-nitrosourea (ENU) have been established to provide comprehensive collections of mouse models, which were then mined and analyzed in phenotype-driven studies. Here, we applied ENU mutagenesis in a high-throughput fashion for a gene-driven identification of new mutations. Selected members of the large superfamily of G protein-coupled receptors (GPCR), melanocortin type 3 (Mc3r) and type 4 (Mc4r) receptors, and the orphan chemoattractant receptor GPR33, were used as model targets to prove the feasibility of this approach. Parallel archives of DNA and sperm from mice mutagenized with ENU were screened for mutations in these GPCR, and *in vitro* assays served as a preselection step before *in vitro* fertilization was performed to generate the appropriate mouse model. For example, mouse models for inherited obesity were established by selecting fully or partially inactivating mutations in Mc4r. Our technology described herein has the potential to provide mouse models for a GPCR dysfunction of choice within <4 mo and can be extended to other gene classes of interest.

alleles; ethylnitrosourea/pharmacology; heterozygote; mice; mutants/pharmacology; mutation

GENE-TARGETING DISRUPTION TECHNIQUES have evolved into efficient tools in unveiling gene function (50). More than 2,500 individual genes have been targeted in mice to study the phenotypical consequences. Although gene-targeting methods are well established, it is still a time-consuming and expensive approach. Additionally to gene targeting and gene trap efforts, chemical random mutagenesis techniques with the germ line supermutagen *N*-ethyl-*N*-nitrosourea (ENU) were established to provide comprehensive collections of mouse models. Although historically, ENU mutagenesis has been carried out in a high-throughput fashion for phenotype-driven studies (23, 35, 41), it can also be used for a gene-driven identification of functional relevant mutations (2, 9, 10, 12, 32, 38, 41, 42). Compared with gene-targeting techniques, the ENU-based ap-

proach has several advantages in respect of costs and time. Once the allele of interest is retrieved mouse generation can be finished within 2 mo, whereas embryonic stem cell-based approaches vary highly in performance and can take up to 1 yr to create a heterozygous carrier.

We have recently described an ENU-based parallel C3HeB/FeJ sperm and DNA archive containing 17,000 samples and ~340,000 independent alleles (2). Detection of mutations within a gene of interest can be performed with temperature gradient capillary electrophoresis (TGCE) in a high-throughput fashion. 93% of all sperm samples in our archive have a quality that is sufficient for *in vitro* fertilization (IVF) and allow a retrieval rate of >90% (2). To test the feasibility of an ENU-based gene-targeting approach, we applied this technology on several genes coding for members of the G protein-coupled receptor (GPCR) superfamily. The completion of the human and other mammalian genome sequencing projects has identified >1,000 genes that belong to the GPCR superfamily. Two-thirds of these genes are thought to encode odorant receptors. Of the remaining ~440 receptors in the mouse genome (Batch data/sequence retrieval service provided by ENSEMBL, <http://www.ensembl.org/>), the natural ligand has been identified for approximately half of these receptors, leaving >200 so-called “orphan” GPCRs with no known ligand or function (16). To date ~120 GPCRs have been pharmacologically targeted (22, 25), which makes them the target for >60% of all currently prescribed drugs. Therefore, understanding the function of orphan GPCRs becomes a task of paramount importance in academic and industrial research. Consequently, pharmacological and functional genomic strategies are being employed to identify activating ligands and their functional relevance.

As proof of principle we first targeted two well-characterized GPCRs for melanocyte-stimulating hormones (MSH), the melanocortin receptors types 3 and 4, MC3R and MC4R. Several functional relevant mutations were identified in our sperm archive, and two different mutations in the mouse MC4R were chosen for mouse generation. Mutant MC4R mice displayed an adipose phenotype as found in mice generated with the traditional gene-targeting technique (24). In a next step, we established a procedure to successfully use this method even for orphan GPCR.

EXPERIMENTAL PROCEDURES

High-Throughput Mutation Detection With TGCE

Parallel archives of sperm and DNA of ENU-mutagenized mice have been generated as described elsewhere (2). Heterozygous DNA

Article published online before print. See web site for date of publication (<http://physiolgenomics.physiology.org>).

Address for reprint requests and other correspondence: M. Augustin, Ingenium Pharmaceuticals AG, Fraunhoferstr. 13, 82152 Martinsried, Germany (e-mail: martin.augustin@ingenium-ag.com).

was used to amplify 12 overlapping PCR fragments corresponding to the three GPCR, *Mc3r*, *Mc4r*, and *Gpr33*. Length of fragments ranged from 297 to 499 bp. Heteroduplex analysis was performed essentially as described (30) on 96- or 192-capillary SCE9610 genetic analyzer platforms (SpectruMedix LLC, State College). Two standard run protocols with temperature gradients ranging from 55 to 60°C and 60 to 65°C were used to account for major differences in the G/C content of the fragments analyzed. The electrophoretic pattern was digitally recorded and analyzed using CheckMate software (SpectruMedix LLC, State College). Fragments with peak patterns different from wild-type control have been sequenced for validation and to determine the nature of the mutation. DNA sequencing was performed by cycle sequencing with BigDye terminators on ABI3700 sequencing devices (Applied Biosystems).

Generation of Receptor Constructs

Mutant alleles were cloned from *Mus musculus* C3HeB/FeJ genomic DNA (*Mc3r*, *Mc4r*, and *Gpr33* are intron-less in the coding region) and inserted into the eukaryotic expression vector pcDps. For immunologic detection purposes wild-type and mutant *Mc3r*, *Mc4r*, and *Gpr33* constructs were tagged with an NH₂-terminal hemagglutinin-derived 9-amino acid epitope (YPYDVPDYA, HA tag) and a COOH-terminal FLAG epitope (DYKDDDDK) downstream of the initiating start codon and upstream of the termination codon, respectively, using a PCR-based site-directed mutagenesis and restriction fragment replacement strategy. All PCR-derived constructs were verified by DNA sequencing.

To monitor the transfection efficiency and for control purposes in ELISA studies, an expression plasmid (pEGFP-C1 vector; Clontech, Palo Alto, CA) for the green fluorescent protein (GFP) was used.

Second Messenger Assays and ELISA Studies

COS-7 cells were grown in Dulbecco's modified Eagle's medium (DMEM) supplemented with 10% fetal bovine serum, 100 U/ml penicillin, and 100 µg/ml streptomycin at 37°C in a humidified 7% CO₂ incubator. Cells were split into 12-well plates (2 × 10⁵ cells/well) and transiently transfected with the calcium phosphate precipitation method (5 µg of plasmid DNA/well). To measure inositol phosphate (IP) formation, transfected COS-7 cells were incubated with 2 µCi/ml of myo-3H-inositol (18.6 Ci/mmol, Perkin Elmer) for 18 h. Thereafter, cells were washed once with serum-free DMEM containing 10 mM LiCl followed by incubation for 1 h at 37°C. Intracellular IP levels were determined by anion-exchange chromatography as described (5).

For determination of intracellular cAMP cells were seeded into 12-well plates (2 × 10⁵ cells/well) and, 12 h later, transfected with Metafectene (0.25 µg of plasmid DNA/well and 1.25 µl Metafectene; Biontex Laboratories, Munich, Germany). Two days after transfection cells were labeled with 2 µCi/ml of [³H]adenine (31.7 Ci/mmol; Pharmacia, Freiburg, Germany). The next day the cAMP assay was performed. First, cells were washed once with serum-free DMEM containing 1 mM 3-isobutyl-1-methylxanthine (IBMX; Sigma, Steinheim, Germany) to remove nonincorporated [³H]adenine. Then, cells were incubated in the presence of increasing amounts of endogenous agonists (α-MSH, β- or γ-MSH; 0.1–1,000 nM in DMEM plus 1 mM IBMX), a synthetic agonist (NDP-α-MSH; 0.01–100 nM in DMEM plus 1 mM IBMX), or without agonist (only DMEM plus 1 mM IBMX) for 1 h at 37°C. Intracellular cAMP was released by incubation of 1 ml of 5% trichloric acid and was measured by anion exchange chromatography as described (43). Cyclic AMP accumulation data were analyzed with the GraphPad Prism program (GraphPad Software, San Diego, CA).

To estimate cell surface expression of receptors carrying an NH₂-terminal HA tag, we used an indirect cellular ELISA (44), further referred to as "surface ELISA." Briefly, COS-7 cells were seeded into 48-well plates (2.5 × 10⁴ cells/well) and transfected (0.2 µg of

DNA/well and 0.8 µl of Metafectene/well, Biontex Laboratories). After 72 h cells were formaldehyde-fixed without disrupting the cell membrane and incubated with a biotin-labeled anti-HA monoclonal antibody (1 µg/ml 12CA5; Roche, Molecular Biochemicals). Bound anti-HA antibody was then detected with the help of a peroxidase-labeled streptavidin conjugate (0.2 µg/ml, Sigma). After removal of excess unbound conjugate, H₂O₂ and o-phenylenediamine (2.5 mM each in 0.1 M phosphate-citrate buffer, pH 5.0) were added to serve as substrate and chromogen, respectively. After 15 min the enzyme reaction was stopped by the addition of 1 M H₂SO₄ containing 0.05 M Na₂SO₃, and color development was measured bichromatically at 492 and 620 nm using a plate reader (Sunrise, Tecan).

To further assess the amounts of full-length HA/FLAG double-tagged Gpr33 constructs and to demonstrate that the reduction of cell surface expression levels is not due to a decrease of receptor expression in general, a previously developed "sandwich ELISA" was used (44). In brief, transfected cells were harvested from 6-cm dishes, and membrane preparations were solubilized in lysis buffer (10 mM Tris·HCl, pH 7.4, 150 mM NaCl, 1 mM DTT, 1 mM EDTA, 1% desoxycholate, 1% Nonidet P-40, 0.2 mM PMSF, 10 µg/ml aprotinin) overnight. Microtiter plates (Maxi Sorp, Nunc Immuno plates, Nunc) were coated with a monoclonal antibody directed against the COOH-terminal FLAG tag (10 µg/ml in 0.05 M borate buffer, M2 antibody; Sigma). After incubation with the membrane solubilisates, bound full-length Gpr33 proteins were detected with the combination of a biotin-labeled anti-HA monoclonal antibody (12CA5, Roche Molecular Biochemicals) and a peroxidase-labeled streptavidin conjugate (see above).

Mouse Generation and Characterization

IVF was performed using one straw of the identified sperm sample in conjunction with either C3HeB/FeJ or C57BL/6J oocytes. A minimum of 45 two-cell embryos were transferred into two or three pseudopregnant foster females (strain CD1). Offspring of the mixed background were used to obtain heterozygous breeder pairs to produce homozygous animals. Mice were genotyped by PCR analysis of mouse tail DNA using standard PCR conditions (94°C for 1 min/62°C for 1 min/72°C for 2 min, 35 cycles). For genotyping of the Y302C and I194F *Mc4r* mouse strains the primers pairs 5'-GGA TCC CCA GAG CTT CAC CG-3'/5'-GAC TAG TCA CTT AAT ACC TGC TAG-3' and 5'-GGA TCC CCA GAG CTT CAC CG-3'/5'-GAA CAT GGA AAT GAG GCA GAT CA-3' (degenerated base is underlined) were used, respectively. PCR products were digested with Bsp1286I for Y302C and with BspHI for I194F and separated on 2% agarose gels. Animals were maintained in a controlled animal facility with 25°C room temperature, 60% humidity, and a 12-h light/12-h dark cycle.

RESULTS

GPCR as Targets for Gene-Driven ENU Mutagenesis

GPCR are optimal targets for gene-driven mutagenesis studies as their complete open reading frame (ORF) can be screened by analyzing a limited number of fragments. Although <5% of murine genes lack introns in their protein coding regions, most GPCR are intron-less at least in their coding regions (19, 33). We assessed the number of fragments necessary to perform mutation screens on 444 individual non-odorant GPCR selected from the ENSEMBL database. For this subset of receptors detailed gene structure and ORF information is available. If overlapping PCR fragments of a maximal length of 500 bp are used to cover the complete ORF, analysis of 75% of all GPCR can be performed in three to four fragments, and 95% of all GPCR can be screened in five fragments, respectively.

Table 1. Screening/Mutations results obtained by TGCE

Gene Symbol	Accession Number	Length CDS	Number of Fragments Screened	Coding Mbp Screened	Mutations Found	Missense Mutations	Silent Mutations	Mutations (n) per Mb	Missense Mutations (n) per Mb
<i>Gpr33</i>	NM_008159	1,020	4	9.55	6	5	1	0.63	0.52
<i>Mc3r</i>	NM_008561	972	5	9.10	3	3		0.33	0.33
<i>Mc4r</i>	NM_016977	999	4	9.36	6	5	1	0.64	0.53

TGCE, temperature gradient capillary electrophoresis; CDS, coding sequence; Mbp, megabase pair; Mc3r; melanocortin type 3 receptor; Mc4r, melanocortin type 4 receptor.

To prove that ENU mutagenesis delivers valuable mutations of interest in GPCR, we used TGCE to screen a nonredundant subset of our DNA archive representing 9,367 DNA samples for mutations in the *Mc3r*, *Mc4r*, and *Gpr33* genes. TGCE is fast and cost effective and has the utility for mutation discovery analysis (2, 20, 30, 34, 42). Twenty-eight megabase pairs (Mbp) of coding sequence were screened, and 15 mutations (13 missense, 2 silent) were identified (Tables 1 and 2). This translates into an overall ratio of 1 missense mutation in every 2.33 Mbp or 2,162 individuals analyzed and is in good agreement with the data reported for other large archives of ENU-mutagenized mouse DNA and sperm (2, 9, 10, 38, 42).

Functional Analysis of *Mc3r* and *Mc4r* Variants

Melanocortin receptors are activated by pro-opiomelanocortin derived peptides α - and β -MSH and by highly potent synthetic ligand NDP- α -MSH. They signal through activation of the G_s/adenylyl cyclase pathway (17, 18). Wild-type *Mc3r*, *Mc4r*, and all mutants identified (see Table 2) were investigated for cell surface expression and signal transduction properties following stimulation with NDP- α -MSH, α -MSH, and β -MSH. Additionally, *Mc3r* constructs were stimulated with γ -MSH.

Functional characterization of wild-type and mutant *Mc3r*. Three missense mutations of *Mc3r* (Y152C, L247Q, and T267P; Table 2) were functionally analyzed. First, COS-7 cells were transfected with wild-type and mutant receptors and then agonist-induced cAMP formation was determined. As shown in Table 3, efficacies (E_{max} values) of agonists were reduced for Y152C, L247Q, and T267P compared with wild type. EC₅₀ values of different agonists at Y152C and L247Q showed no

significant changes (Table 3). To further analyze the molecular mechanism that causes the impaired receptor function, we performed ELISA studies. This ELISA assay allows receptor quantification at the cell surface independent from its binding ability. As shown in Table 3, Y152C and L247Q display a reduced cell surface expression, whereas T267P leads to an almost complete intracellular retention of the mutant receptor protein. In summary, the most prominent loss-of-function phenotype was found for T267P, which would therefore be the choice for generation of a *Mc3r*-deficient mouse model.

Functional characterization of wild-type and mutant *Mc4r*. Five missense mutations were identified in *Mc4r*: Y21H, R147S, I194F, M281R, and Y302C (Table 2). Maximum agonist stimulations of Y21H, R147S, and I194F were comparable to the wild-type receptor (Table 3). M281R showed reduced and Y302C almost no signal transduction efficacy following agonist incubation (Table 3). However, determination of α - and β -MSH potencies on R147S, M281R, and I194F revealed EC₅₀ values shifted toward higher agonist concentrations (Table 3). It is of interest to note that NDP- α -MSH potency at M281R and I194F was unchanged, indicating that both mutations did not interfere with the binding site of the synthetic agonist. Y21H had no effect on receptor function (Table 3). Cell surface expression of Y21H, R147S, and I194F was comparable to the wild-type, whereas cell surface expression of M281R and Y302C was significantly reduced (Table 3). For mouse generation, at least two different types of *MC4R* dysfunction, partial (I194F, M281R) and complete (Y302C) loss of function can be considered.

Generation and phenotypical characterization of two mouse lines carrying mutations in *Mc4r*. To correlate the results from the in vitro characterization of mutant GPCR with the in vivo phenotype, we chose two functionally different *Mc4r* mutations, I194F and the functionally inactive Y302C, for mouse generation. Mouse lines were established in the C3HeB/FeJ/C57BL/6J 50/50% mixed background, and littermates of all three genotypes were compared with respect to their body weight. In consensus with the expected adipose phenotype, homozygous mutant mice of both strains displayed a significant increase in body weight compared with wild-type mice, suggesting that a 100-fold reduced potency of α -MSH at I194F (see Table 3) cannot be compensated for in vivo (Supplementary Table 1 online and Fig. 1; the online version of this article contains supplemental data).

In both strains the weight gain is more pronounced in females than in males. Interestingly, the obesity is more severe and develops earlier in mice homozygous for the Y302C mutation than in those homozygous for I194F (Supplementary Table 1 online). This suggests that the residual activity of I194F is sufficient to alleviate the weight gain to some degree.

Table 2. Types of mutation found within the archive

Gene Symbol	Nucleotide Change	Amino Acid Change	Localization in Protein
<i>Mc3r</i>	A to G	Y152C	ICL2
	T to A	L247Q	TMD6
	A to C	T267P	TM6/ECL3
<i>Mc4r</i>	T to C	Y21H	NH ₂ terminus
	C to T (silent)	D37D	NH ₂ terminus
	G to T	R147S	TMD3/ICL2
	A to T	I194F	TMD5
	T to A	M281K	TMD7
	A to G	Y302C	TMD7
<i>Gpr33</i>	A to T	I122F	TMD3
	T to C (silent)	R126R	TMD3
	C to T	R147W	TMD4
	A to T	Q151L	TMD4
	C to A	T196K	ECL2
	T to A	Y225N	TMD5

ICL, intracellular loop; ECL, extracellular loop; TMD, transmembrane domain.

Table 3. Functional characterization of wild-type and mutant melanocortin receptors

Gene Symbol	Amino Acid Change	NDP- α -MSH		α -MSH		β -MSH		γ -MSH		Cell Surface Expression, % WT
		E_{max} , % WT	EC_{50} , nM	E_{max} , % WT	EC_{50} , nM	E_{max} , % WT	EC_{50} , nM	E_{max} , % WT	EC_{50} , nM	
<i>Mc3r</i>	WT	100	1.6 \pm 0.2	100	2.8 \pm 1.0	100	71.6 \pm 66.3	100	7.2 \pm 1.2	100
	Y152C	45.1 \pm 1.8	4.0 \pm 1.9	48.5 \pm 11.3	4.4 \pm 2.5	76.9 \pm 11.6	175.4 \pm 90.5	68.8 \pm 16.0	16.6 \pm 1.7	92.3 \pm 3.7
	L247Q	44.0 \pm 11.3	1.5 \pm 0.3	42.3 \pm 0.1	5.0 \pm 2.0	82.9 \pm 2.6	36.8 \pm 1.2	63.6 \pm 1.5	14.2 \pm 5.9	73.3 \pm 11.2
	T267P	17.7 \pm 3.9	n.d.	n.d.	n.d.	31.0 \pm 5.8	n.d.	21.4 \pm 1.6	n.d.	27.6 \pm 4.6
<i>Mc4r</i>	WT	100	0.5 \pm 0.3	100	1.6 \pm 0.1	100	7.8 \pm 2.8	n.d.	n.d.	100
	Y21H	107.3 \pm 36.6	0.2 \pm 0.1	96.0 \pm 20.2	1.2 \pm 0.4	99.8 \pm 0.1	2.1 \pm 0.7	n.d.	n.d.	97.0 \pm 1.8
	R147S	69.2 \pm 8.9	5.3 \pm 1.4	62.6 \pm 0.6	59.7 \pm 5.8	79.3 \pm 14.1	161.0 \pm 13.5	n.d.	n.d.	94.9 \pm 3.2
	M281R	55.3 \pm 10.9	0.8 \pm 0.3	40.9 \pm 6.2	76.2 \pm 6.0	63.7 \pm 23.0	276.0 \pm 73.8	n.d.	n.d.	44.4 \pm 12.9
	I194F	102.7 \pm 1.7	0.6 \pm 0.4	129.4 \pm 0.7	104.6 \pm 0.8	110.2 \pm 1.7	325.5 \pm 121.6	n.d.	n.d.	105.1 \pm 7.4
	Y302C	20.7 \pm 3.0	n.d.	20.9 \pm 0.6	n.d.	16.6 \pm 0.1	n.d.	n.d.	n.d.	64.9 \pm 10.2

To evaluate the functional properties of wild-type (WT) and mutant *Mc3r* and *Mc4r*, receptor efficacy (E_{max}) and potency (EC_{50}) were determined from concentration-response curves of endogenous (α -, β -, or γ -MSH) and synthetic (NDP- α -MSH) agonists (for details see EXPERIMENTAL PROCEDURES). Data are presented as means \pm SE of 3 or 4 independent experiments, each carried out in duplicate. Cell surface expression levels of melanocortin receptors were measured by indirect cellular ELISA. Specific optical density (OD) readings [OD value of hemagglutinin (HA)-tagged construct minus OD value of green fluorescent protein (GFP)-transfected cells] are given as percentage of WT HA-tagged *Mc3r* and *Mc4r*. The nonspecific OD value (GFP) was 0.19 ± 0.04 , and the OD value of the WT HA-tagged *Mc3r* was 1.33 ± 0.17 and of the WT HA-tagged *Mc4r* was 1.00 ± 0.08 . ELISA data are given as means \pm SD of 2 or 3 independent experiments, each carried out in quadruplicate. MSH; melanocyte-stimulating hormone; n.d., not determined.

Heterozygotes of the Y302C mouse line develop an intermediate phenotype, indicating a codominant mode of inheritance. In contrast, the weight gain in heterozygous I194F animals is very close to that of the homozygotes (Fig. 1).

Characterization of the *Gpr33* Mutants

Mouse models deficient for orphan receptors are useful tools to address their physiological relevance. In contrast to GPCR where the natural agonist is known, the selection procedure of

mutations found in an ENU-based mutagenesis approach in orphan receptor genes is most challenging. Therefore, we have chosen *Gpr33* to test a procedure that helps in selecting functionally relevant mutations even in orphan GPCR. GPR33 is a chemoattractant-like GPCR that was previously identified as a pseudogene in humans (31). We have recently shown that *Gpr33* became coincidentally inactivated in humans, great apes, and some rodents within the last 0.8 million years, which suggests a selective pressure on this chemoattractant receptor

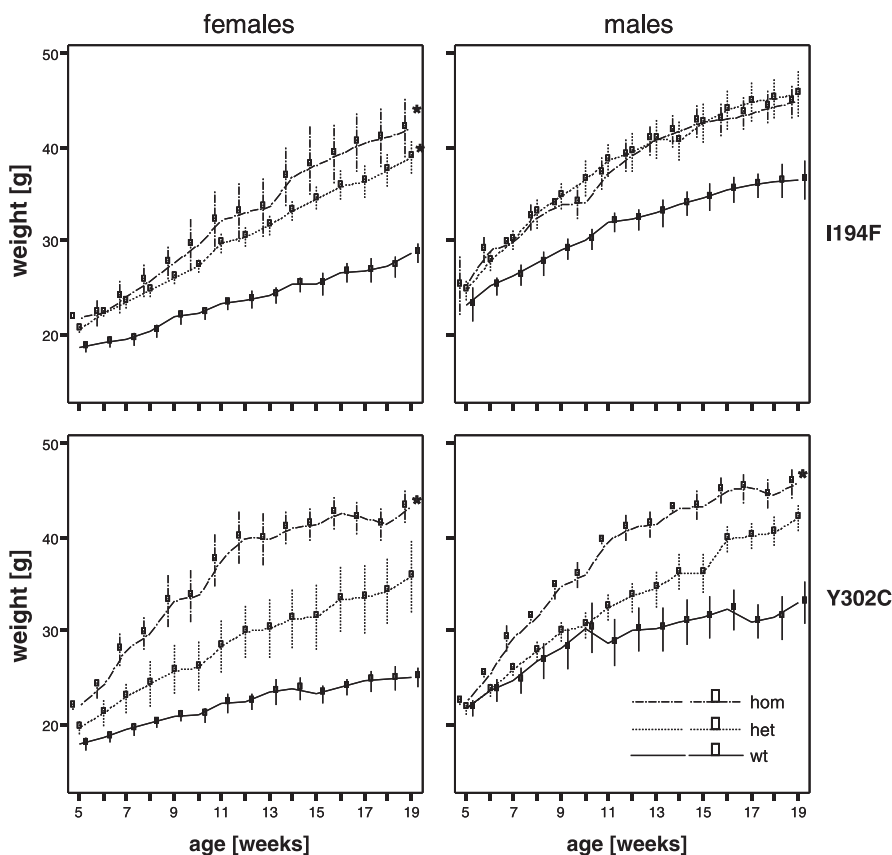


Fig. 1. Weight gain of melanocortin type 3 receptor (*Mc4r*)-mutant mice and wild-type (wt) littermates. Littermates of the 3 genotypes of mouse lines I194F (top) and Y302C mice (bottom) were weighed weekly. A general linear model for repeated measures was applied separately to both sexes. het, Heterozygous. $P < 0.05$ in all panels except for the males of I194F for which a trend was detected ($P = 0.062$); $n \geq 5$ for all genotypes except the homozygous (hom) females of the I194F ($n = 3$); *significant difference to wt mice (post hoc Scheffé's test; $P < 0.05$). Data are means \pm SE.

in these species (40). It is of interest to note that ~2.5% of the human population still harbor the ancient intact allele of *Gpr33*. To analyze the functional relevance of *Gpr33*, a knock-out animal model that normally carries a functional *Gpr33* would be advantageous. Our sequence analysis of the DNA archive revealed five missense mutations in the coding sequence of *Gpr33*: I122F, R147W, Q151L, T196K, and Y225N (Table 2).

Phylogenetic Conservation of Affected Positions in GPR33

First we utilized an evolutionary approach to evaluate the potential relevance of the mutagenized positions in *Gpr33*. This approach is based on the assumption that residues that are required for global receptor structure, agonist binding, and signal transduction were kept constant during evolution (46). The sequence information of >120 mammalian GPR33 orthologs cloned so far (40) enabled us to determine the conservation of each mutated residue (Fig. 2). The positions Ile¹²² and Tyr²²⁵ were found to be 100% conserved among all GPR33 orthologs. It is of interest that Tyr²²⁵ is conserved not only in GPR33 but also in a large number of GPCR of family A. Less conservation is found for Arg¹⁴⁷ (30%, naturally replaced by Cys, Gly, Ser, Gln, Asn, Ile in other species) and Gln¹⁵¹ (naturally replaced by Gly, Val, Arg in other species) and Thr¹⁹⁶ (naturally replaced by Ile, Lys, Ala, Pro in other mammalian *Gpr33* orthologs) (Fig. 2).

Functional Analysis of GPR33

Most chemoattractant and chemokine-like GPCR mediate their signal transduction via coupling to G_{i/o} proteins that inhibit adenylyl cyclases and, therefore, decrease intracellular cAMP levels (48). According to the current model of GPCR function, receptor overexpression can result in constitutive activation of signaling pathways. Thus coupling abilities of several receptors, including orphan receptors, have been characterized by overexpression even in the absence of agonist (46).

Because of the low sensitivity of cAMP inhibition, “gain-of-function” assays have been developed to determine signaling of G_{i/o}-coupled receptors. It has been demonstrated that replacement of the four or five COOH-terminal amino acids of Gα_q with the corresponding Gα_i residues confers the ability to stimulate the phospholipase C-β pathway onto G_i-coupled receptors (11). The specificity and sensitivity of chimeric proteins such as Gα_{qi4} can be improved by further modifications (lack of the NH₂-terminal extension, introduction of an NH₂-terminal consensus site for myristoylation), further referred to as Gα_{Δ6qi4myr} (28). As shown in Fig. 2A, basal activity of the human P2Y₁₂, a well-characterized G_i-coupled GPCR (46), and the murine GPR33 were ~7- and 4.6-fold increased, respectively, when compared with GFP-transfected cells. However, none of the mutant GPR33 showed a significant elevation of basal IP levels in transfected COS-7 cells (Fig. 3A). To further analyze whether the loss of basal activity is due to a reduction or lack of receptor expression in the cell and/or at the cell surface, immunological studies were performed. Using a sandwich ELISA to measure receptor expression in total cell lysate, we demonstrated that all GPR33 mutants were expressed at almost similar levels compared with the wild-type GPR33 (Fig. 3B). To answer the question whether the altered receptor function is accompanied by a reduction of cell surface expression, we performed an indirect cell surface ELISA. Q151L and T196K were expressed at similar levels compared with the wild-type GPR33, whereas I122F and R147W displayed only 35–45% cell surface expression. Y225N was almost completely retained in the cellular interior (Fig. 3B). In summary, our data favor I122F, R147W, and Y225N for generation of a GPR33-deficient mouse model.

DISCUSSION

Mutagenesis with the germline supermutagen ENU has been carried out in a high-throughput fashion for the generation of large numbers of new mutants for systematic studies of mammalian gene function. Although this concept is generally accepted for phenotype-driven screens, there are two major concerns about the application of ENU mutagenesis in gene-driven approaches: 1) the generation of the desired allele (in most cases a constitutive or somatic loss of function) cannot be presupposed and 2) the phenotypic consequences of the generated mutations can be difficult to predict. Nevertheless, gene-driven random mutagenesis has major advantages compared with existing technologies, as for example gene targeting. In particular, the investigations of orphan genes will profit from the application of this technology, as targeted knockouts frequently only uncover the first step in development where the mutated gene is absolutely required. In contrast point mutations may provide additional information due to hypomorphic

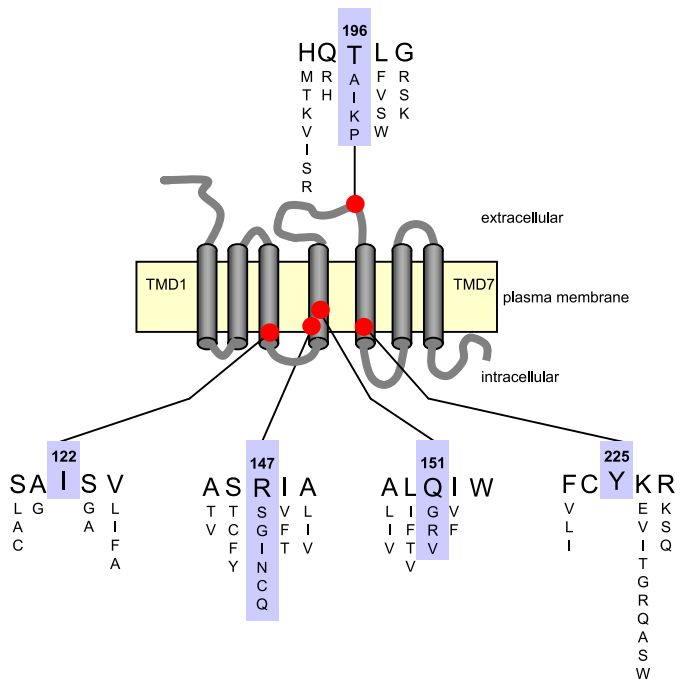


Fig. 2. Localization and evolutionary conservation of amino acid positions mutated in *Gpr33*. The 7 transmembrane domains (TMDs) and loops of *Gpr33* are depicted, and the approximate positions of missense mutations are indicated (red circle). The amino acid sequences shown in large letters correspond to the murine *Gpr33* sequence. Comparison of amino acid sequences of over 120 mammalian *Gpr33* orthologs deposited in GenBank (40) revealed high conservation of positions Ile¹²² and Tyr²²⁵, whereas positions Arg¹⁴⁷, Gln¹⁵¹ and Thr¹⁹⁶ are substituted by other amino acids in different mammals.

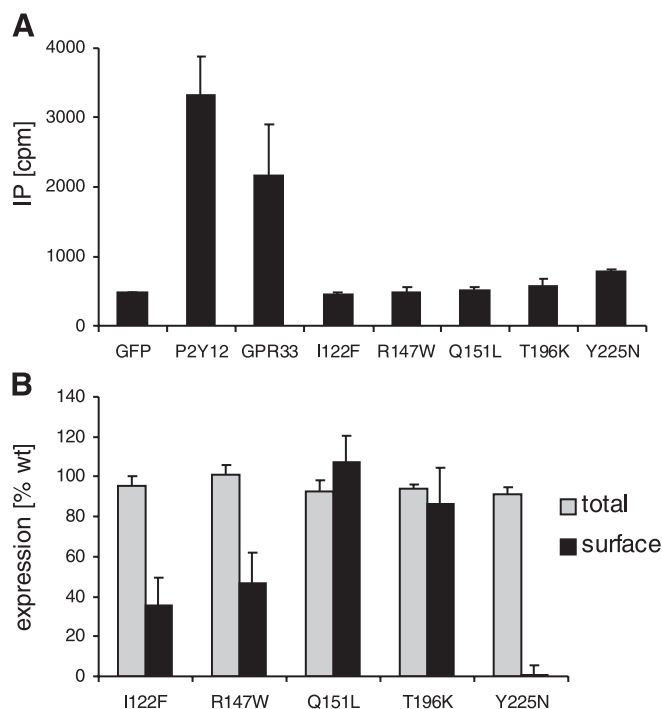


Fig. 3. Functional characterization of wt and mutant GPR33 receptors. **A:** determination of the basal receptor activity. The human ADP receptor P2Y12 (positive control), the wt and the mutant GPR33 constructs were coexpressed with the chimeric $G\alpha_{\Delta 6q14myr}$ protein in COS-7 cells, and inositol phosphate (IP) assays were performed as described (EXPERIMENTAL PROCEDURES). As a negative control, a plasmid encoding green fluorescent protein (GFP) was cotransfected with $G\alpha_{\Delta 6q14myr}$. Basal IP formations are shown (cpm/well). Data are presented as means \pm SE of 2 independent experiments, each carried out in triplicate. **B:** cell surface expression levels of the GPR33 mutant receptors measured by indirect cellular ELISA. Specific optical density (OD) readings [OD value of hemagglutinin (HA)-tagged GPR33 construct minus OD value of GFP-transfected cells] are given as a percentage of wt HA-tagged GPR33. The nonspecific OD value (GFP) was 0.02 ± 0.01 , and the OD value of the wt HA-tagged GPR33 was 0.57 ± 0.09 . ELISA data are given as means \pm SD of 2 independent experiments, each carried out in quadruplicate. Total cellular expression levels of the GPR33 mutant receptors measured by sandwich ELISA. Specific OD readings (OD value of HA-tagged GPR33 construct minus OD value of GFP-transfected cells) are given as a percentage of wt HA/FLAG-tagged GPR33. The nonspecific OD value (GFP) was 0.03 ± 0.01 , and the OD value of the wt GPR33 was 1.36 ± 0.19 . Sandwich ELISA data are given as means \pm SE of 2 independent experiments, each carried out in quadruplicate.

changes, partial loss or even gain of function. In addition, models can be generated after their allele discovery in the DNA archive from their corresponding sperm archive, in parallel and in matter of weeks by a simple IVF step. Here, we use GPCR to show that appropriate *in vivo* assays allows prioritization and characterization of mutations obtained by ENU random mutagenesis before *in vitro* fertilization. The receptor variants obtained provide a broader view into the target gene's physiological role than the mere complete loss of function would do. In this study three GPCR, two well-characterized (*Mc3r* and *Mc4r*) and one orphan receptor (*Gpr33*), have been analyzed, and 15 mutations were identified in total. This number was obtained by screening only 50% of our parallel DNA/sperm archive (9,367 samples), whereas our current archive size is 19,000. Furthermore, eight out of the total of 15 mutations identified cause severe impairments in signal transduction properties. In MC3R, T267P showed a complete loss of func-

tion probably due to intracellular retention. This residue is conserved among MC3R, MC4R, and MC5R and located within the COOH-terminal portion of transmembrane helix 6. One can speculate that proline, as a helical kink-producing residue, may lead to a premature termination of the α -helical character of transmembrane domain 6 at its COOH-terminal end. So far only one MC3R mutation, I183N, identified in an obese patient (29), results in a complete loss of function (39).

Currently ~ 50 predominantly heterozygous mutations of the human MC4R are known to be associated with early onset obesity or morbid obesity of adults. These mutations have recently been classified on the basis of their functional consequences, namely abrogated membrane expression, altered activation by agonists, or decreased constitutive activity (21). Due to the heterogeneity of the genetic background and the environmental influences these classes and the residual activity determined *in vitro* is not clearly associated with the time of onset or the severity of the obesity.

Besides obesity, MC4R mutations cause an increase in body length and lean mass (53), and all three features are represented in the MC4R knockout mouse (24). Both hyperphagia and hypometabolism contribute to the altered energy homeostasis, and both effects are mediated via different but MC4R-dependent neuronal pathways. The paraventricular nucleus of the hypothalamus is involved in the hyperphagia but does not play a role in regulating the metabolic rate (4). Another common feature between the human syndrome and the mouse model is hyperinsulinemia (15, 24). Early pharmacological studies have shown that peripheral administration of α -MSH resulted in increased plasma glucose, glucagon, and insulin levels (26, 27). In contrast, chronic central administration in rats enhanced the insulin sensitivity of liver and peripheral tissues (36). Moreover, the MC4R has been suggested to be involved in binge eating and mood disorders, immunomodulation, regulation of bone formation, and triglyceride metabolism (6, 7, 8, 13, 47). Activation of the MC4R modulates erectile function and sexual behavior (52). Large efforts were undertaken to develop highly potent MC4R ligands to treat erectile dysfunction (3). For this issue our mouse models are potentially highly valuable.

It is conceivable that a partial loss of MC4R function affects the physiological processes listed above to different degrees, and the study of these pleiotropic aspects might be facilitated by mouse models bearing a mutant MC4R with some residual function, thus closely resembling the common human situation.

Four (R147S, I194F, M281R, Y302C) of five identified mouse *Mc4r* mutations affect positions that are highly conserved during MC4R evolution. Sequence analysis of over 40 mammalian orthologs (H. Römpler, P. Tarnow, H. Biebermann, T. Schöneberg, unpublished results) revealed 100% conservation of these four positions. These mutations resulted either in partial (R147S, I194F, M281R) or complete (Y302C) loss of receptor function. Two of these mutations, R147S and Y302C, were found in the DRY motif and NP(X)_nY motif, respectively. Consistent with our findings, the mutated positions are thought to play an important functional role in most rhodopsin-like GPCR (1, 37, 51). Two mutations (I194F, M281R) interfered with function of the natural agonists α - and β -MSH, but potency of the synthetic agonist NDP- α -MSH was not altered. Partial loss of GPCR function is a frequent cause of GPCR-related diseases (45). Here, patients may benefit from

(synthetic) agonists with binding abilities not impaired by the specific mutation. For example, the human MC4R mutation S127L resulted in a partial loss of function when stimulated with α -MSH (14, 49) but is comparable to wild-type receptor function after NDP- α -MSH challenge in vitro (P. Tarnow, A. Elnser, H. Krude, A. Grüters, H. Biebermann, unpublished observations). The investigated mouse Mc4R mutation I194F of this study is comparable to the human MC4R S127L mutation.

To date, there are no animal models available to test the feasibility of this therapeutic approach, and ENU-based mutagenesis may be a fast and convenient tool to provide such mouse models. To test whether NDP- α -MSH is able to substitute for the abrogated effect of the endogenous ligands in vivo, we generated I194F mutant mice and, for comparison, mice bearing the functionally inactive mutation Y302C. Initial phenotyping of these mice showed an obesity that is more pronounced and develops earlier in the Y302C homozygotes than in those bearing the I194F mutation. This suggests that the residual receptor activity of the I194F line is sufficient to alleviate the phenotype to some degree. This modulation of the obesity demonstrates that the in vitro data translate into the in vivo phenotype, at least in this case. In humans, large studies are necessary to elaborate correlations between MC4R function and the severity of the obese phenotype, as the condition is caused by a multitude of environmental and genetic factors. Nevertheless, it has been shown that the obesity due to *Mc4r* mutations is inherited in a codominant mode (15). Similarly, Y302C heterozygous mice showed a weight gain intermediate between wild-type and homozygotes. Interestingly, the differences between heterozygotes and homozygotes of the I194F line were much smaller and statistically not significant, suggesting that the altered signaling capacity of this mutation causes a nearly dominant inheritance.

Identification of the physiological role of functionally uncharacterized genes is a challenging task to which ENU-induced mouse mutants can contribute valuable insights. Even in the case of unknown natural agonists, the combination of different agonist-independent functional assays allows for an interpretation and selection of inactivating missense mutations in orphan GPCR. The first evidence comes from structural comparison of receptor orthologs. It is reasonable to assume that mutations of highly conserved residues may alter receptor function. Indeed, analysis of over 90 inactivation missense mutations in the V2 vasopressin receptor revealed that >80% of all inactivating missense mutations are found at positions that are evolutionary conserved among V2 vasopressin receptor orthologs (45). In GPR33, I122F and Y225N affect positions that are 100% conserved. As shown in Fig. 3A, basal activity is a natural property of the murine wild-type GPR33. All mutations tested abolished this function. Because all mutant receptors are equally expressed within the cell, the loss of basal activity in case of I122F, R147W, and Y225N is probably due to an altered cell surface expression. Although Arg¹⁴⁷ is less conserved, the introduction of a bulky Trp residue may interfere with proper receptor trafficking. On the basis of our current characterization data, the functional relevance of Q151L and T196K cannot be finally evaluated. In summary, three (I122F, R147W, and Y225N) out of five missense mutation found in this mutational screen present more than one piece of evidence of an altered receptor function, at least in

vitro. To our knowledge there is no report that a mutant GPCR that displays an altered function in these in vitro assays still properly functions in vivo. Because of overexpression many mutant GPCR display some signal transduction abilities in in vitro assays that cannot be verified in vivo. Therefore, these three mutations can be selected for the generation of murine models deficient for GPR33 function. Finally, a *Gpr33*-deficient mouse model carrying the Y225N mutation was established and is under current investigation. As expected from its polymorphic (intact and pseudogenic) existence in humans and great apes (40), *Gpr33* deficiency neither is lethal nor has obvious effects on mouse fertility, on gross morphologic development, on size, weight, and macroscopy of major organs, or on differential blood cell counts (unpublished data). Because *Gpr33* is mainly expressed in macrophages, specific tests of their cellular functions and challenging in infection models may help to delineate its functional relevance.

In conclusion, we successfully used an ENU-based mutagenesis approach in combination with a set of functional assays for generation of GPCR-deficient mouse models. In addition to advantages in time and costs of mouse generation, the ENU-based mutagenesis approach is suitable for addressing the physiological relevance of orphan GPCR as well as for generation of GPCR mutants, not only with a complete loss of function but also with more distinct functional alterations.

Access to the Archive

Using Ingenium's parallel archive to develop selected models requires specific know-how and equipment for high-throughput DNA analysis and specialized expertise in IVF procedures. Ingenium provides high-throughput DNA analysis and IVF support for individual academic researchers on request. Supplementary information is available through Ingenium's website: www.ingenium-ag.com.

ACKNOWLEDGMENTS

We thank Deborah Simon for critical reading of the manuscript. Present addresses: J. Grosse, Paradigm Therapeutics Ltd., 162 Cambridge Science Park, Cambridge, CB4 0GP, UK; D. Korthaus: Institute of Laboratory Animal Science and Austrian Center for Biomodels and Transgenetics, University of Veterinary Medicine, Vienna, Austria.

GRANTS

This work was supported by the Deutsche Forschungsgemeinschaft (Sfb 577), Bundesministerium für Bildung und Forschung (NGFN-2, TP13), the European FP6 program Diabetesity, and Fonds der Chemischen Industrie.

REFERENCES

1. Acharya S and Karnik SS. Modulation of GDP release from transducin by the conserved Glu134-Arg135 sequence in rhodopsin. *J Biol Chem* 271: 25406–25411, 1996.
2. Augustin M, Sedlmeier R, Peters T, Huffstadt U, Kochmann E, Simon D, Schöniger M, Garke-Mayerthaler S, Laufs J, Mayhaus M, Franke S, Klose M, Graupner A, Kurzmann M, Zinser C, Wolf A, Voelkel M, Kellner M, Kilian M, Seelig S, Koppius A, Teubner A, Korthaus D, Nehls M, and Wattler S. Efficient and fast targeted production of murine models based on ENU mutagenesis. *Mamm Genome* 16: 405–413, 2005.
3. Bakshi RK, Hong Q, Olson JT, Ye Z, Sehat IK, Weinberg DH, MacNeil T, Kalyani RN, Tang R, Martin WJ, Strack A, McGowan E, Tamvakopoulos C, Miller RR, Stearns RA, Tang W, MacIntyre DE, van der Ploeg LH, Patchett AA, and Nargund RP. 1-Amino-1,2,3,4-tetrahydronaphthalene-2-carboxylic acid as a Tic mimetic: application in the synthesis of potent human melanocortin-4 receptor selective agonists. *Bioorg Med Chem Lett* 15: 3430–3433, 2005.

4. Balthasar N, Dalggaard LT, Lee CE, Yu J, Funahashi H, Williams T, Ferreira M, Tang V, McGovern RA, Kenny CD, Christiansen LM, Edelstein E, Choi B, Boss O, Aschkenasi C, Zhang CY, Mountjoy K, Kishi T, Elmquist JK, and Lowell BB. Divergence of melanocortin pathways in the control of food intake and energy expenditure. *Cell* 123: 493–505, 2005.
5. Berridge MJ. Rapid accumulation of inositol trisphosphate reveals that agonists hydrolyse polyphosphoinositides instead of phosphatidylinositol. *Biochem J* 212: 849–858, 1983.
6. Bohm M, Eickelmann M, Li Z, Schneider SW, Oji V, Diederichs S, Barsh GS, Vogt A, Stieler K, Blume-Peytavi U, and Luger TA. Detection of functionally active melanocortin receptors and evidence for an immunoregulatory activity of alpha-melanocyte-stimulating hormone in human dermal papilla cells. *Endocrinology* 146: 4635–4646, 2005.
7. Bronner G, Sattler AM, Hinney A, Soufi M, Geller F, Schafer H, Maisch B, Hebebrand J, and Schaefer JR. The 103I variant of the melanocortin 4 receptor (MC4R) is associated with low serum triglyceride levels. *J Clin Endocrinol Metab* 91: 535–538, 2006.
8. Chaki S and Okuyama S. Involvement of melanocortin-4 receptor in anxiety and depression. *Peptides* 26: 1952–1964, 2005.
9. Coghill EL, Hugill A, Parkinson N, Davison C, Glenister P, Clements S, Hunter J, Cox RD, and Brown SD. A gene-driven approach to the identification of ENU mutants in the mouse. *Nat Genet* 30: 255–256, 2002.
10. Concepcion D, Seburn KL, Wen G, Frankel WN, and Hamilton BA. Mutation rate and predicted phenotypic target sizes in ethylnitrosourea-treated mice. *Genetics* 168: 953–959, 2004.
11. Conklin BR, Farfel Z, Lustig KD, Julius D, and Bourne HR. Substitution of three amino acids switches receptor specificity of Gq alpha to that of Gi alpha. *Nature* 363: 274–276, 1993.
12. Culiati CT, Klebig ML, Liu Z, Monroe H, Stanford B, Desai J, Tandan S, Hughes L, Kerley MK, Carpenter DA, Johnson DK, Rinchik EM, and Li Q. Identification of mutations from phenotype-driven ENU mutagenesis in mouse chromosome 7. *Mamm Genome* 16: 555–566, 2005.
13. Dumont LM, Wu CS, Tatnell MA, Cornish J, and Mountjoy KG. Evidence for direct actions of melanocortin peptides on bone metabolism. *Peptides* 26: 1929–1935, 2005.
14. Elsner A, Tarnow P, Schaefer M, Ambrugger P, Krude H, Gruters A, and Biebermann H. MC4R oligomerizes independently of extracellular cysteine residues. *Peptides* 27: 372–379, 2006.
15. Farooqi IS, Keogh JM, Yeo GS, Lank EJ, Cheetham T, and O'Rahilly S. Clinical spectrum of obesity and mutations in the melanocortin 4 receptor gene. *N Engl J Med* 348: 1085–1095, 2003.
16. Foord SM. Receptor classification: post genome. *Curr Opin Pharmacol* 2: 561–566, 2002.
17. Gantz I, Konda Y, Tashiro T, Shimoto Y, Miwa H, Munzert G, Watson SJ, DelValle J, and Yamada T. Molecular cloning of a novel melanocortin receptor. *J Biol Chem* 268: 8246–8250, 1993.
18. Gantz I, Miwa H, Konda Y, Shimoto Y, Tashiro T, Watson SJ, DelValle J, Yamada T, and Munzert G. Molecular cloning, expression, and gene localization of a fourth melanocortin receptor. *J Biol Chem* 268: 15174–15179, 1993.
19. Gentles AJ and Karlin S. Why are human G-protein-coupled receptors predominantly intronless? *Trends Genet* 15: 47–49, 1999.
20. Giraldo-Rosa W, Vleugels RA, Musiek AC, and Sligh JE. High-throughput mitochondrial genome screening method for nonmelanoma skin cancer using multiplexed temperature gradient capillary electrophoresis. *Clin Chem* 51: 305–311, 2005.
21. Govaerts C, Srinivasan S, Shapiro A, Zhang S, Picard F, Clement K, Lubrano-Berthelie C, and Vaisse C. Obesity-associated mutations in the melanocortin 4 receptor provide novel insights into its function. *Peptides* 26: 1909–1919, 2005.
22. Hopkins AL and Groom CR. The druggable genome. *Nat Rev Drug Discov* 1: 727–730, 2002.
23. Hrade de Angelis MH, Flaszinkel H, Fuchs H, Rathkolb B, Soewarto D, Marschall S, Heffner S, Pargent W, Wuensch K, Jung M, Reis A, Richter T, Alessandrini F, Jakob T, Fuchs E, Kolb H, Kremmer E, Schaeble K, Rollinski B, Roscher A, Peters C, Meitinger T, Strom T, Steckler T, Holsboer F, Klopstock T, Gekeler F, Schindewolf C, Jung T, Avraham K, Behrendt H, Ring J, Zimmer A, Schughart K, Pfeffer K, Wolf E, and Balling R. Genome-wide, large-scale production of mutant mice by ENU mutagenesis. *Nat Genet* 25: 444–447, 2000.
24. Huszar D, Lynch CA, Fairchild-Huntress V, Dunmore JH, Fang Q, Berkemeier LR, Gu W, Kesterson RA, Boston BA, Cone RD, Smith FJ, Campfield LA, Burn P, and Lee F. Targeted disruption of the melanocortin-4 receptor results in obesity in mice. *Cell* 88: 131–141, 1997.
25. Klabunde T and Hessler G. Drug design strategies for targeting G-protein-coupled receptors. *ChemBiochem* 3: 928–944, 2002.
26. Knudtson J. Alpha-melanocyte stimulating hormone increases plasma levels of glucagon and insulin in rabbits. *Life Sci* 34: 547–554, 1984.
27. Knudtson J, Johansen PW, Haug E, and Gautvik K. Effects of hypersecretion of growth hormone and prolactin on plasma levels of glucagon and insulin in GH3-cell-tumor-bearing rats, and the influence of bromocriptine treatment. *Life Sci* 39: 617–621, 1986.
28. Kostenis E. Is Galphal6 the optimal tool for fishing ligands of orphan G-protein-coupled receptors? *Trends Pharmacol Sci* 22: 560–564, 2001.
29. Lee YS, Poh LK, and Loke KY. A novel melanocortin 3 receptor gene (MC3R) mutation associated with severe obesity. *J Clin Endocrinol Metab* 87: 1423–1426, 2002.
30. Li Q, Liu Z, Monroe H, and Culiati CT. Integrated platform for detection of DNA sequence variants using capillary array electrophoresis. *Electrophoresis* 23: 1499–1511, 2002.
31. Marchese A, Nguyen T, Malik P, Xu S, Cheng R, Xie Z, Heng HH, George SR, Kolakowski LF Jr, and O'Dowd BF. Cloning genes encoding receptors related to chemoattractant receptors. *Genomics* 50: 281–286, 1998.
32. Michaud EJ, Culiati CT, Klebig ML, Barker PE, Cain KT, Carpenter DJ, Easter LL, Foster CM, Gardner AW, Guo ZY, Houser KJ, Hughes LA, Kerley MK, Liu Z, Olszewski RE, Pinn I, Shaw GD, Shipcock SG, Wymore AM, Rinchik EM, and Johnson DK. Efficient gene-driven germ-line point mutagenesis of C57BL/6J mice. *BMC Genomics* 6: 164, 2005.
33. Minneman KP. Splice variants of G protein-coupled receptors. *Mol Interv* 1: 108–116, 2001.
34. Murphy K, Hafez M, Philips J, Yarnell K, Gutshall K, and Berg K. Evaluation of temperature gradient capillary electrophoresis for detection of the factor v leiden mutation : coincident identification of a novel polymorphism in factor v. *Mol Diagn* 7: 35–40, 2003.
35. Nolan PM, Peters J, Strivens M, Rogers D, Hagan J, Spurr N, Gray IC, Vizer L, Brooker D, Whitehill E, Washbourne R, Hough T, Greenaway S, Hewitt M, Liu X, McCormack S, Pickford K, Selley R, Wells C, Tymowska-Lalanne Z, Roby P, Glenister P, Thornton C, Thaug C, Stevenson JA, Arkell R, Mburu P, Hardisty R, Kiernan A, Erven A, Steel KP, Voegeling S, Guenet JL, Nickols C, Sadri R, Nasse M, Isaacs A, Davies K, Browne M, Fisher EM, Martin J, Rastan S, Brown SD, and Hunter J. A systematic, genome-wide, phenotype-driven mutagenesis programme for gene function studies in the mouse. *Nat Genet* 25: 440–443, 2000.
36. Obici S, Feng Z, Tan J, Liu L, Karkanias G, and Rossetti L. Central melanocortin receptors regulate insulin action. *J Clin Invest* 108: 1079–1085, 2001.
37. Okada T, Ernst OP, Palczewski K, and Hofmann KP. Activation of rhodopsin: new insights from structural and biochemical studies. *Trends Biochem Sci* 26: 318–324, 2001.
38. Quwailid MM, Hugill A, Dear N, Vizer L, Wells S, Horner E, Fuller S, Weedon J, McMath H, Woodman P, Edwards D, Campbell D, Rodger S, Carey J, Roberts A, Glenister P, Lalanne Z, Parkinson N, Coghill EL, McKeone R, Cox S, Willan J, Greenfield A, Keays D, Brady S, Spurr N, Gray I, Hunter J, Brown SD, and Cox RD. A gene-driven ENU-based approach to generating an allelic series in any gene. *Mamm Genome* 15: 585–591, 2004.
39. Rached M, Buronfosse A, Begeot M, and Penhoat A. Inactivation and intracellular retention of the human I183N mutated melanocortin 3 receptor associated with obesity. *Biochim Biophys Acta* 1689: 229–234, 2004.
40. Römpler H, Schulz A, Pitra C, Coop G, Przeworski M, Paabo S, and Schöneberg T. The rise and fall of the chemoattractant receptor GPR33. *J Biol Chem* 280: 31068–31075, 2005.
41. Russ A, Stumm G, Augustin M, Sedlmeier R, Wattler S, and Nehls M. Random mutagenesis in the mouse as a tool in drug discovery. *Drug Discov Today* 7: 1175–1183, 2002.
42. Sakuraba Y, Sezutsu H, Takahashi KR, Tsuchihashi K, Ichikawa R, Fujimoto N, Kaneko S, Nakai Y, Uchiyama M, Goda N, Motoi R, Ikeda A, Karashima Y, Inoue M, Kaneda H, Masuya H, Minowa O, Nouguchi H, Toyoda A, Sakaki Y, Wakana S, Noda T, Shiroishi T, and Gondo Y. Molecular characterization of ENU mouse mutagenesis and archives. *Biochem Biophys Res Commun* 336: 609–616, 2005.
43. Salomon Y, Londos C, and Rodbell M. A highly sensitive adenylate cyclase assay. *Anal Biochem* 58: 541–548, 1974.

44. Schoneberg T, Schulz A, Biebermann H, Gruters A, Grimm T, Hubschmann K, Filler G, Gudermann T, and Schultz G. V2 vasopressin receptor dysfunction in nephrogenic diabetes insipidus caused by different molecular mechanisms. *Hum Mutat* 12: 196–205, 1998.
45. Schoneberg T, Schulz A, Biebermann H, Hermsdorf T, Rompler H, and Sangkuhl K. Mutant G-protein-coupled receptors as a cause of human diseases. *Pharmacol Ther* 104: 173–206, 2004.
46. Schulz A and Schoneberg T. The structural evolution of a P2Y-like G-protein-coupled receptor. *J Biol Chem* 278: 35531–35541, 2003.
47. Tao YX and Segaloff DL. Functional analyses of melanocortin-4 receptor mutations identified from patients with binge eating disorder and nonobese or obese subjects. *J Clin Endocrinol Metab* 90: 5632–5638, 2005.
48. Thelen M. Dancing to the tune of chemokines. *Nat Immun* 2: 129–134, 2001.
49. Valli-Jaakola K, Lipsanen-Nyman M, Oksanen L, Hollenberg AN, Kontula K, Bjorbaek C, and Schalin-Jantti C. Identification and characterization of melanocortin-4 receptor gene mutations in morbidly obese Finnish children and adults. *J Clin Endocrinol Metab* 89: 940–945, 2004.
50. Vanhaesebroeck B, Rohn JL, and Waterfield MD. Gene targeting: attention to detail. *Cell* 118: 274–276, 2004.
51. Wess J. Molecular basis of receptor/G-protein-coupling selectivity. *Pharmacol Ther* 80: 231–264, 1998.
52. Wessells H, Blevins JE, and Vanderah TW. Melanocortinergic control of penile erection. *Peptides* 26: 1972–1977, 2005.
53. Yeo GS, Farooqi IS, Aminian S, Halsall DJ, Stanhope RG, and O'Rahilly S. A frameshift mutation in MC4R associated with dominantly inherited human obesity. *Nat Genet* 20: 111–112, 1998.

